A&A 613, L8 (2018)
https://doi.org/10.1051/0004-6361/201833144

Astronomy & Astrophysics

LETTER TO THE EDITOR

The VMC survey*

XXX. Stellar proper motions in the central parts of the Small Magellanic Cloud

F. Niederhofer[1], M.-R. L. Cioni[1], S. Rubele[2,3], T. Schmidt[1], K. Bekki[4], R. de Grijs[5,6], J. Emerson[7], V. D. Ivanov[8,9], M. Marconi[10], J. M. Oliveira[11], M. G. Petr-Gotzens[9], V. Ripepi[10], J. Th. van Loon[11], and S. Zaggia[2]

[1] Leibniz-Institut für Astrophysik Potsdam, An der Sternwarte 16, 14482 Potsdam, Germany
e-mail: fniederhofer@aip.de
[2] Osservatorio Astronomico di Padova - INAF, Vicolo dell'Osservatorio 5, 35122 Padova, Italy
[3] Dipartimento di Fisica e Astronomia, Università di Padova, Vicolo dell'Osservatorio 2, 35122 Padova, Italy
[4] ICRAR, M468, University of Western Australia, 35 Stirling Hwy, 6009 Crawley, Western Australia, Australia
[5] Department of Physics and Astronomy, Macquarie University, Balaclava Road, Sydney, NSW 2109, Australia
[6] International Space Science Institute-Beijing, 1 Nanertiao, Zhongguancun, Hai Dian District, Beijing 100190, PR China
[7] Astronomy Unit, School of Physics and Astronomy, Queen Mary University of London, Mile End Road, London E1 4NS, UK
[8] European Southern Observatory, Ave. Alonso de Cordova 3107, Vitacura, Santiago, Chile
[9] European Southern Observatory, Karl-Schwarzschild-Str. 2, 85748 Garching bei München, Germany
[10] INAF - Osservatorio Astronomico di Capodimonte, via Moiariello 16, 80131, Naples, Italy
[11] Lennard-Jones Laboratories, Keele University, ST5 5BG, UK

Received 2 April 2018 / Accepted 24 April 2018

ABSTRACT

We present the first spatially resolved map of stellar proper motions within the central (~3.1 × 2.4 kpc) regions of the Small Magellanic Cloud (SMC). The data used for this study encompasses four tiles from the ongoing near-infrared VISTA survey of the Magellanic Clouds system and covers a total contiguous area on the sky of ~6.81 deg^2. Proper motions have been calculated independently in two dimensions from the spatial offsets in the K_s filter over time baselines between 22 and 27 months. The reflex motions of approximately 33 000 background galaxies are used to calibrate the stellar motions to an absolute scale. The resulting catalog is composed of more than 690 000 stars which have been selected based on their position in the $(J - K_s, K_s)$ color-magnitude diagram. For the median absolute proper motion of the SMC, we find $(\mu_\alpha \cos(\delta), \mu_\delta)$ = (1.087 ± 0.192 (sys.) ± 0.003 (stat.), −1.187 ± 0.008 (sys.) ± 0.003 (stat.)) mas yr^{-1}, consistent with previous studies. Mapping the proper motions as a function of position within the SMC reveals a nonuniform velocity pattern indicative of a tidal feature behind the main body of the SMC and a flow of stars in the south-east moving predominantly along the line-of-sight.

Key words. proper motions – surveys – galaxies: individual: SMC – Magellanic Clouds – stars: kinematics and dynamics

1. Introduction

The Large and the Small Magellanic Cloud (LMC and SMC) are the most prominent dwarf galaxy satellites of the Milky Way and are in the early phases of a minor merger event. Tidal interactions between the two Clouds led to the formation of the gaseous Magellanic Stream (see e.g., Nidever et al. 2008; D'Onghia & Fox 2016) and the Magellanic Bridge (e.g., Irwin et al. 1985) which is composed of stars and gas, and connects the two dwarf galaxies. Thanks to their close vicinity, the Clouds provide a unique opportunity for detailed studies of the stellar kinematics within an interacting pair of galaxies. However, for a long time, the one dimensional (1D) line-of-sight velocities of stars have been the only source of dynamical information. With accurate proper motion measurements now available using modern, ground- and space-based observing facilities, it is now possible to assess the full three-dimensional (3D) velocity field of stellar populations, both as a function of age and position within the Magellanic Clouds. Measurements of stellar proper motions using the *Hubble* Space Telescope (HST) have changed the traditional picture; that is, that the Magellanic Clouds have orbited the Milky Way several times. Kallivayalil et al. (2006a,b, 2013) showed that both satellites move faster around our Galaxy than originally thought. This implies that the Clouds are rather on a first passage or a long period orbit, depending on the mass of the Milky Way and the LMC (e.g., Besla et al. 2007; Patel et al. 2017). The internal proper motion field of the LMC, which was measured by van der Marel & Kallivayalil (2014) for the first time, reveals a clockwise rotation of the LMC disk in the plane of the sky, consistent with previous line-of-sight velocity measurements. This result was confirmed by van der Marel & Sahlmann (2016) using the proper motions from the *Tycho-Gaia* Astrometric Solution (TGAS) Catalog (Michalik et al. 2015; Lindegren et al. 2016). The SMC, on the other hand, seems to have a more complex kinematical structure. Radial velocity measurements of intermediate-age red giant branch (RGB) stars show signs of tidal stripping in the outer regions of the SMC and a velocity gradient along the northwest-southeast axis (Dobbie et al. 2014). The young stellar populations also show such velocity gradient,

* Based on observations made with VISTA at the Paranal Observatory under program ID 179.B-2003.

as well as a higher velocity towards the SMC Wing, a horizontal extension of the SMC towards the east (Evans & Howarth 2008).

Here we present, for the first time, a large-scale map of stellar proper motions within the central ~31 × 2.4 kpc of the SMC, covering a total contiguous sky area of ~6.81 deg^2. The data for this study stem from the multi-epoch near-infrared (NIR) VISTA survey of the Magellanic Clouds system (VMC, Cioni et al. 2011). Our group has already analyzed some individual VMC tiles to measure the proper motions of stars within the LMC (Cioni et al. 2014), SMC (Cioni et al. 2016) and the Galactic globular cluster 47 Tuc (Cioni et al. 2016; Niederhofer et al. 2018).

2. Observations and photometry

The data used in this study are taken with the Visible and Infrared Survey Telescope for Astronomy (VISTA, Sutherland et al. 2015) and comprise four VISTA tiles, namely SMC 4_3, 4_4, 5_3 and 5_4. Each tile is composed of six individual pawprint images with specific offsets, in order to observe a continuous area on the sky, owing to the gaps between the 16 VIRCAM detectors in the field of view (Emerson et al. 2006). In the stacked tile, each object is observed at least twice, whereas a small fraction can be observed up to six times. In two narrow stripes at the edge of a tile, sources are only observed once. Each tile corresponds to 1.77 deg^2 on the sky. The tiles that cover the SMC are arranged such that stripes of single observations within a tile overlap with adjacent tiles in a north-south direction. Therefore, the area covered by the four VMC tiles is ~6.81 deg^2. The VMC survey plan includes multiple observations of each VMC tile, with three epochs in the Y and J band and 12 epochs in the K_s filter (whereas one epoch per filter is split into two shallow exposures), spread over a mean period of two years. For the calculation of the proper motions within the four SMC tiles, we use only the observations in the K_s filter (central wavelength 2.15 μm) to minimize problems with differential atmospheric diffraction. We have time baselines of 23 months for SMC 4_3, 27 months for SMC 4_4, 22 months for SMC 5_3, and 24 months for SMC 5_4. Details of the tiles used here are given in Table 1. The astrometry of VISTA pawprints shows a systematic pattern of the order of 10−20 mas coming from residual World Coordinate System errors. This effect limits the precision of proper-motion measurements of single objects but our overall results are in good agreement with recent studies suggesting that there is no large systematic offset in the astrometry.

For the proper motion calculations, we used pawprint images at individual epochs which were reduced and calibrated with the VISTA Data Flow System (VDFS) pipeline v1.3 (Irwin et al. 2004; González-Fernández et al. 2018) and retrieved from the VISTA Science Archive[1] (VSA, Cross et al. 2012). We performed point spread function (PSF) photometry on each of these images separately, as described by Rubele et al. (2015). We also created a deep multi-band catalog which will be used in the following. For this, we performed PSF photometry on deep tile images where individual pawprints from all epochs were homogenized to have a constant reference PSF and then combined to a single tile (see Rubele et al. 2015). Finally, we cross-matched the catalogs in all bands using a 1″ matching radius.

3. The proper motion field of the SMC

We calculate the proper motions of stars within the four VMC tiles covering the central parts of the SMC for each detector and pawprint separately to minimize systematic effects when combining different pawprints. The method to determine the proper motions is described in detail by Niederhofer et al. (2018). We followed these steps for each tile separately. Briefly, we first cross-correlated the individual detection catalogs from the different epochs with the deep multi-band catalog using a matching radius of 0.″5 to remove spurious detections. We then identified sources that are most likely background galaxies based on several selection criteria involving the position in the color-color diagram and the sharpness of the source (see Niederhofer et al. 2018). We also selected only well measured galaxies with photometric uncertainties of <0.1 mag in the K_s filter. Our final list of background galaxies within all four tiles contains ~54 900 galaxies. Subsequently, we transformed the x and y detector positions of the sources in the catalogs from all epochs to a common reference frame in order to compensate for small pointing differences. As the reference epoch, to which all other epochs were transformed, we chose the ones with the best seeing conditions (between 0.″76 and 0.″83). We performed the transformation in two stages. First, we used the sample of galaxies, which are assumed to be at rest, to perform an initial transformation and then used the stars themselves for a more refined transformation. For both steps, we chose a general fit geometry, allowing for a shift, rotation, and scaling in two directions. After inspection of the results of the transformations, we decided to remove two epochs for tiles SMC 4_3 and SMC 4_4 and one epoch for tile SMC 5_3 since these epochs had systematically higher residuals in the transformation, most likely due to larger seeing or airmasses during the observations. We calculated the proper motions of the stars and the reflex motions of the galaxies by fitting a linear least-squares regression model independently to the x and y positions of each source on the detector chip which has been detected in all epochs as a function of the Mean Julian Date. The resulting slope gives the proper motion of the source in pixels day^{-1} which was then transformed to mas yr^{-1}. Finally, we corrected the motions of the stars by the mean residual reflex motion of the galaxies within each tile, to put the proper motions on an absolute scale. Our final proper motion catalogs consist of ~1 770 000 stars and ~33 000 galaxies of which ~760 000 and ~17 000, respectively, are unique sources.

To get a cleaner sample of stars belonging only to the SMC, we selected stars that fall within various regions in the $(J - K_s, K_s)$ color-magnitude diagram (CMD) which are dominated by SMC populations (see Fig. 1). Specifically, we selected stars within regions A and B (young main sequence stars), E (lower RGB stars), G (supergiants), I and N (red supergiants), J (red clump stars), K (upper RGB stars) and M (asymptotic giant branch stars). We further constrained our sample by selecting stars with photometric errors $\sigma(K_s) \leq 0.05$ mag. Using these selections, our final SMC proper motions catalog contains ~1 590 000 entries (~690 000 individual sources). We find a median proper motion of the SMC of $(\mu_\alpha \cos(\delta), \mu_\delta)$ = (1.087 ± 0.192, −1.187 ± 0.008) mas yr^{-1} which is consistent within the uncertainties with previous ground-based measurements (Vieira et al. 2010; Costa et al. 2011) but larger in the RA direction compared to space-based (Kallivayalil et al. 2013; van der Marel & Sahlmann 2016) measurements. The quoted uncertainties are the systematic errors which we estimated from the median deviations of the stellar proper motions from zero before correcting for the galaxies' reflex motion. We note that the uncertainties in the RA direction are considerably larger than the ones in the Dec direction. This can be explained by the fact that also Milky Way stars have been used for the transformation to a common reference frame. The proper motions of these stars

[1] http://horus.roe.ac.uk/vsa

Table 1. Overview of the VMC tiles used for this study and the proper motion results.

Tile	Central coordinates		Position Angle	Number	Time baseline	Number	$\mu_\alpha\cos(\delta)$	μ_δ
	RA_{J2000} (deg)	Dec_{J2000} (deg)	(deg)	of epochs	(months)	of SMC stars	(mas yr^{-1})	(mas yr^{-1})
SMC 4_3	11.3112	−73.1198	−1.1369	11	23	641 397	0.537 ± 0.101	−1.172 ± 0.014
SMC 4_4	16.3303	−73.0876	+3.6627	11	27	429 048	1.201 ± 0.174	−0.680 ± 0.029
SMC 5_3	11.2043	−72.0267	−1.2392	12	22	220 678	1.761 ± 0.304	−1.724 ± 0.054
SMC 5_4	16.1088	−71.9975	+3.4514	13	24	295 996	1.625 ± 0.325	−1.508 ± 0.010
Total						1 587 119	1.087 ± 0.192	−1.187 ± 0.008

Notes. The uncertainties refer to the systematic errors, the statistical errors are of the order of 0.003−0.009 mas yr^{-1} per tile in both directions.

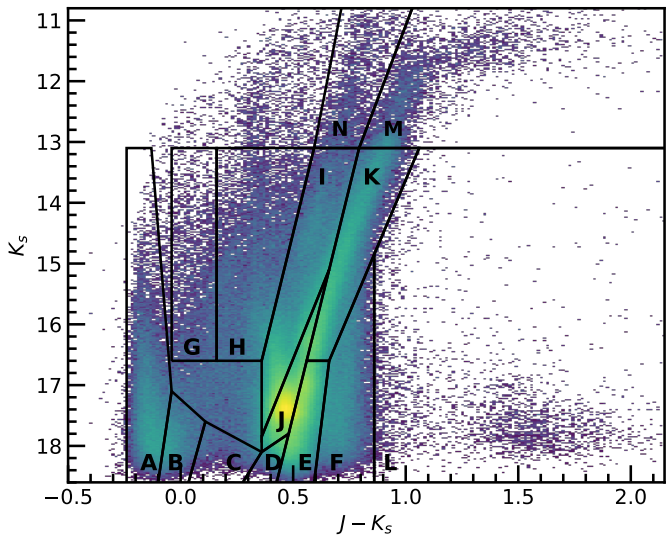

Fig. 1. Stellar density (Hess) diagram in the $(J-K_s, K_s)$ color-magnitude space of all sources with proper motions measurements. Overplotted as black polygons are regions of different stellar populations as defined by Cioni et al. (2016) and El Youssoufi et al. (in prep.), the latter adding regions M and N and extending regions A and L.

are comparable to the ones in the SMC in the Dec direction but larger by a factor of ∼5−10 in the RA direction. Owing to the vast numbers of stars, the statistical uncertainty is of the order of 0.003 mas yr^{-1} in both directions.

For a spatially resolved map of proper motions within the SMC, we divided the total area covered by the four VMC tiles into a 20×20 grid (bin size ∼18 700 pc^2) and calculated the median proper motion within each grid cell. Figure 2 shows the resulting map, where the vectors represent the direction and magnitude of the median motion within each bin. A stellar density map of sources detected by the VMC survey is also displayed in the background. The map is centered at the optical center of the SMC ($\alpha_{2000} = 00^h52^m12^s.5$, $\delta_{2000} = -72°49'43''$, de Vaucouleurs & Freeman 1972). Two different patterns of motion are evident from the overall velocity map. Stars in the outer regions of the SMC to the north and southeast uniformly move towards the Southeast, whereas the velocity vector of stars located in the main body of the SMC, where the stellar density is highest, has a significantly ($>3\sigma$) smaller component in the RA direction (see also Table 1) and is therefore oriented more towards the south. Additionally, there seems to be a decrease in the absolute value of the velocity when going towards the Magellanic Bridge region to the south-east of the SMC.

4. Discussion and conclusions

Diaz & Bekki (2012) presented dynamical N-body models of the SMC to study, in detail, the kinematical history and the tidal features that arise from the interaction with the LMC and the Milky Way. Their simulations suggest that the formation of the Magellanic Bridge was accompanied by the appearance of another tidal feature which was named "Counter Bridge" by the authors. In their model, this new feature is expected to originate behind the center of the SMC, where we find proper motions with a small RA component, and follow an arc-like structure, whereas most of the Counter Bridge is aligned with the SMC along the line-of-sight. The exact course of the Counter Bridge, however, is still debated but it likely extends towards the north-east of the SMC (Muller & Bekki 2007). The Counter-Bridge can reveal itself as an elongation of the SMC in the radial direction up to about 85 kpc. Ripepi et al. (2017) argued that the 3D distribution of Classical Cepheids within the SMC is elongated and consistent with the model by Diaz & Bekki (2012). The different proper motion signature in regions of highest stellar densities, compared to those in the outer regions of the SMC, can be interpreted in the light of the Counter Bridge. In Fig. 2, the resulting vectors are the median motions of individual stars within each bin. This means that the proper motion signal from stars originating from the Counter Bridge is superimposed on the one from stars associated with the main body of the SMC. For the proper motion vectors to be almost vertical, a contribution of stars with motions in the RA direction opposite to the bulk motion of the SMC is required (see right-hand panel in Fig. 2). Our results would then imply that the stars at the base of the Counter Bridge first move towards the west before they turn towards the north-east. Another possibility would be that the stars which move predominately towards the west are associated with the Western Halo, a tidal feature in the south-west of the SMC, suggested by Dias et al. (2016).

An alternative scenario is that the parts of the SMC with the highest stellar density have motions intrinsically different from the outer regions which might be in the process of being tidally stripped from the SMC. This model seems to be supported by the recent results from van der Marel & Sahlmann (2016), whose sample of TGAS stars, after subtraction of the center-of-mass motion of the SMC, suggest that the stars in the densest regions systematically move towards the west (see their Fig. 1) whereas stars in the eastern outskirts predominantly move towards the east. This might, however, be a selection effect, since in their study only five of eight stars in total are located in the western part of the SMC. Individual precise proper motion measurements of a larger sample of stars will help discriminate between these two theories. We also note that the fields used to calculate the mean motion of the SMC using HST data are located in the transition region in our map, which might explain the lower value in the RA direction found by Kallivayalil et al. (2013).

In the proper motion map presented here, we also see a decrease in the absolute value of the stellar velocity in the southeast of the SMC, towards the Wing and the Magellanic Bridge. In these regions, Evans & Howarth (2008) and Dobbie et al. (2014) found structures with high positive line-of-sight velocities, indicative of tidal stripping. This might suggest that

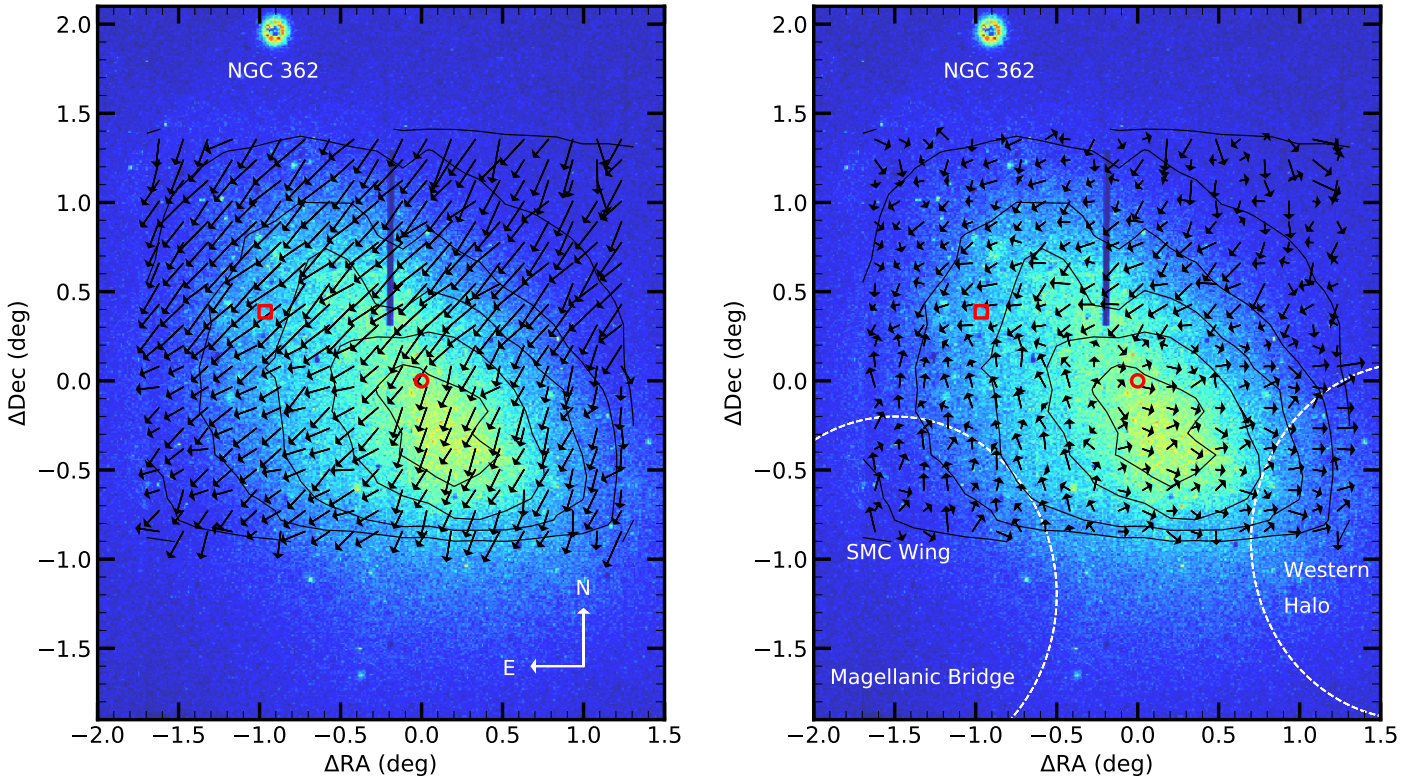

Fig. 2. Proper-motion field (black arrows) of the central regions of the SMC from four tiles of VMC data. The background color image is a density map of objects detected by the VMC. The panel is centered at the optical center of the SMC (red circle) as given by de Vaucouleurs & Freeman (1972), also shown as a red square is the kinematical H I center (Stanimirović et al. 2004). North of the main body of the SMC, the foreground Galactic globular cluster NGC 362 is visible. Black solid lines show density contours of sources for which proper motions have been measured. The contours are at 500, 1500, 3500, 5500, 7500 and 9500 stars per grid cell. The vertical dark stripe at ΔRA∼ −0.2° is due to a narrow gap in the observations. In the left-hand panel, the arrows indicate the observed absolute proper motion, whereas in the right-hand panel, the arrows show the residual proper motions after subtraction of the systemic velocity of the SMC.

the lower proper motion is only a projection effect and that the 3D velocity vector of the stars in these regions is more aligned with the line-of-sight.

In this study we presented, for the first time, a detailed map of stellar proper motions within the central parts of the SMC, showing that the stars do not follow a uniform velocity pattern. In future works, we will extend this study to all VMC tiles covering the SMC, analyze the motions of different stellar populations, and compare the observational results with dynamical *N*-body models to obtain a more complete picture of the stellar motions across the entire SMC.

*Acknowledgements.*Acknowledgements We thank the Cambridge Astronomy Survey Unit and the Wide Field Astronomy Unit in Edinburgh for providing calibrated data products under the support of the Science and Technology Facility Council. This project has received funding from the European Research Council under European Union's Horizon 2020 research and innovation programme (grant agreement No 682115). This research made use of Astropy, a community-developed core Python package for Astronomy (Astropy Collaboration et al. 2013). This study is based on observations obtained with VISTA at the Paranal Observatory under program ID 179.B-2003. We thank the referee for useful comments and suggestions that helped improve the paper.

References

Astropy Collaboration, Robitaille, T. P., Tollerud, E. J., et al. 2013, A&A, 558, A33
Besla, G., Kallivayalil, N., Hernquist, L., et al. 2007, ApJ, 668, 949
Cioni, M.-R. L., Clementini, G., Girardi, L., et al. 2011, A&A, 527, A116
Cioni, M.-R. L., Girardi, L., Moretti, M. I., et al. 2014, A&A, 562, A32
Cioni, M.-R. L., Bekki, K., Girardi, L., et al. 2016, A&A, 586, A77
Costa, E., Méndez, R. A., Pedreros, M. H., et al. 2011, AJ, 141, 136
Cross, N. J. G., Collins, R. S., Mann, R. G., et al. 2012, A&A, 548, A119
de Vaucouleurs, G., & Freeman, K. C. 1972, Vist. Astron., 14, 163
Dias, B., Kerber, L., Barbuy, B., Bica, E., & Ortolani, S. 2016, A&A, 591, A11
Diaz, J. D., & Bekki, K. 2012, ApJ, 750, 36
Dobbie, P. D., Cole, A. A., Subramaniam, A., & Keller, S. 2014, MNRAS, 442, 1663
D'Onghia, E., & Fox, A. J. 2016, ARA&A, 54, 363
Emerson, J., McPherson, A., & Sutherland, W. 2006, The Messenger, 126, 41
Evans, C. J., & Howarth, I. D. 2008, MNRAS, 386, 826
González-Fernández, C., Hodgkin, S. T., Irwin, M. J., et al. 2018, MNRAS, 474, 5459
Irwin, M. J., Kunkel, W. E., & Demers, S. 1985, Nature, 318, 160
Irwin, M. J., Lewis, J., Hodgkin, S., et al. 2004, in Optimizing Scientific Return for Astronomy through Information Technologies, eds. P. J. Quinn, & A. Bridger, Proc. SPIE 5493, 411
Kallivayalil, N., van der Marel, R. P., & Alcock, C. 2006a, ApJ, 652, 1213
Kallivayalil, N., van der Marel, R. P., Alcock, C., et al. 2006b, ApJ, 638, 772
Kallivayalil, N., van der Marel, R. P., Besla, G., Anderson, J., & Alcock, C. 2013, ApJ, 764, 161
Lindegren, L., Lammers, U., Bastian, U., et al. 2016, A&A, 595, A4
Michalik, D., Lindegren, L., & Hobbs, D. 2015, A&A, 574, A115
Muller, E., & Bekki, K. 2007, MNRAS, 381, L11
Nidever, D. L., Majewski, S. R., & Butler Burton W. 2008, ApJ, 679, 432
Niederhofer, F., Cioni, M.-R. L., Rubele, S., et al. 2018, A&A, 612, A115
Patel, E., Besla, G., & Sohn, S. T. 2017, MNRAS, 464, 3825
Ripepi, V., Cioni, M.-R. L., Moretti, M. I., et al. 2017, MNRAS, 472, 808
Rubele, S., Girardi, L., Kerber, L., et al. 2015, MNRAS, 449, 639
Stanimirović, S., Staveley-Smith, L., & Jones, P. A. 2004, ApJ, 604, 176
Sutherland, W., Emerson, J., Dalton, G., et al. 2015, A&A, 575, A25
van der Marel, R. P., & Kallivayalil, N. 2014, ApJ, 781, 121
van der Marel, R. P., & Sahlmann, J. 2016, ApJ, 832, L23
Vieira, K., Girard, T. M., van Altena, W. F., et al. 2010, AJ, 140, 1934